Journal of Earth Science, Vol. 21, No. 5, p. 711–730, October 2010 *ISSN 1674-487X*
Printed in China
DOI: 10.1007/s12583-010-0111-3

Thermal State and Structure of the Lithosphere beneath Eastern China: A Synthesis on Basalt-Borne Xenoliths

Huang Xiaolong (黄小龙), **Xu Yigang*** (徐义刚)
Key Laboratory of Isotope Geochronology and Geochemistry, Guangzhou Institute of Geochemistry, Chinese Academy of Sciences, Guangzhou 510640, *China*

ABSTRACT: Application of reliable thermobarometer on garnet-bearing mantle xenoliths and granulite xenoliths entrained by Cenozoic basalts in eastern China reveals two main types of geotherm. The first type, as exampled by Hannuoba (汉诺坝), Mingxi (明溪) and probably Northeast China, is characterized by constant slope of data in the *P-T* space. The second type, as exampled by the high geotherms of Nüshan (女山) and probably Xinchang (新昌), is characterized by variable slopes, with the samples with pressure <2 MPa defining a slow slope, whereas the samples with pressure >2 MPa define a virtually vertical slope. The different slopes in the second type of geotherm may correspond to different heat transfer mechanisms, with conductive transfer for the shallow upper mantle and advective transfer for the deep mantle. This observed transition in thermal transfer mechanism is consistent with theoretical modeling. The two types of geotherm are not mutually exclusive, because the second type may characterize the thermal state of whole lithospheric section including both mechanical boundary layer (MBL) and thermal boundary layer (TBL), while the first type may only depict the MBL. The variable geotherms for different regions are indicative of a heterogeneous lithospheric structure in eastern China. (a) Eastern North China craton (NCC) is characterized by a second-type geotherm, corresponding to a thin lithosphere (~70 km). Comparison of the equilibrium temperatures of spinel peridotites with this geotherm constrains the depth to Moho in eastern North China craton to be 30 km. In contrast, western NCC (Hannuoba: the first-type geotherm) possesses a relatively low thermal gradient, indicative of a thick lithosphere (>90–100 km) and a thick crust-mantle transition zone. The dramatic change in crustal and mantle structure across the DTGL (Daxing'anling (大兴安岭)-Taihangshan (太行山) gravity lineament) is consistent with recent seismic studies. (b) There is a decrease in thermal gradient and in lithospheric thickness from the coast (Xinchang: the second-type geotherm) to the inland (Mingxi: the first-type geotherm) in South China (from ~80 km to >90 km), which is collaborated with westward variation in basalt geochemistry. (c) The weak convex-upward pattern of the geotherm in Qilin (麒麟) and Leizhou (雷州) Peninsula is peculiar, probably reflecting a transi-

This study was financially supported by the Knowledge Innovation Project of the Chinese Academy of Sciences (No. KZCX2-YW-Q08-3-6), the National Natural Science Foundation of China (Nos. 90714001, 40773015), and the CAS/SAFEA International Partnership Program for Creative Research Teams (No. KZCX2-YW-Q04-06).

*Corresponding author: yigangxu@gig.ac.cn

Manuscript received May 15, 2010.
Manuscript accepted July 1, 2010.

tional feature between conductive and advective heat transfer. It may result from impregnation of mantle plume on the base of the lithosphere. These new results not only provide a basic framework for the ongoing 4-D lithosphere mapping project in eastern China, but also yield important implications for deep processes that operated over the past.

KEY WORDS: geotherm, thermobarometry, garnet-bearing peridotite and pyroxenite, granulite, xenolith, lithosphere, eastern China.

INTRODUCTION

Estimation of equilibrium temperatures and pressures of mantle-derived xenoliths is pivotal to understanding geothermal gradients in the lithosphere and mechanisms of magma generation as well as the depth to important geological transitions such as the crust-mantle and lithosphere-asthenosphere boundaries. Xu Y G et al. (1995) have constructed a thermal gradient for the lithosphere mantle beneath eastern China using estimated equilibrium temperatures and pressures of both spinel and garnet peridotites. Although this geotherm is indicative of extensional setting that is consistent with other geological records of the same region, it also suffered the following shortcomings. (a) In their studies, equilibrium pressures for spinel-facies peridotites were obtained by application of the calibration of $Ca^{Ol\text{-}Cpx}$ barometer by Köhler and Brey (1990). However, the application of this method to natural rocks is hampered by the common Ca-disequilibria between olivine and clinopyroxene due to later thermal event (Werling and Altherr, 1997; Köhler and Brey, 1990) and to lesser extent by the difficulty in precise measurement of Ca content in olivine with an electron microprobe. Moreover, there is a kink along the geotherm, separating the data collected for spinel and garnet peridotites. Given the different barometers used for spinel and garnet facies rocks, the reality of this kink remains unconstrained, because the consistency between different barometers has not been yet demonstrated. (b) Another potential problem associated with the approach used by Xu Y G et al. (1995) is that they tried to define a uniform geotherm for the lithosphere underlying different tectonic unites and large number of localities running from Heilongjiang in Northeast China to Hainan Island in South China (Fig. 1). However, different localities may have different thermal gradients. This is highlighted by recent reconstruction of geotherms (Fig. 2) using xenolith data of Nüshan (Huang et al., 2004; Xu X S et al.,

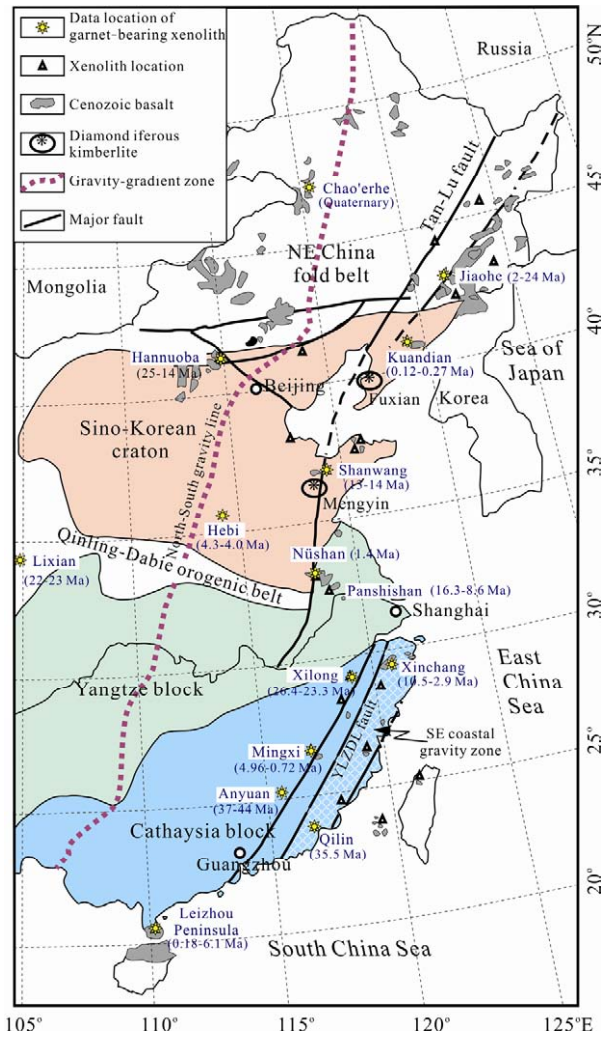

Figure 1. Simplified diagram showing major tectonic units and xenolith location in eastern China. South China is subdivided to inland part and coast part (SE coastal gravity zone) by NNE Yuyao-Lishui (Zhejiang Province), Zhenghe-Dapu (Fujian Province) and Lianhuashan (Guangdong Province) (YLZDL) fault (Ma et al., 2002). Data sources for the ages of host rocks: Lixian (Yu et al., 2005), Leizhou Peninsula, Mingxi, Xinchang, Xilong (Ho et al., 2003), Anyuan (Ye et al., 2001), Nüshan, Shanwang, Hebi, Hannuoba, Kuandian (Liu et al., 1992), Jiaohe (Wang, 1996), Qilin (Huang et al., unpublished data).

1998), Hannuoba (Chen et al., 2001; Shi et al., 2000), Shanwang (Zheng et al., 2006), Kuandian (Fang and Ma, 1998), Jiaohe (Yu, 2008), Chao'erhe (Fan et al., 2008), Mingxi (Lin et al., 1999; Xu X S et al., 1998), Xinchang (Lin et al., 1995), Qilin (Xu Y G et al., 1999, 1996) and Leizhou Peninsula (Lin et al., 2003; Yu et al., 2003). Nevertheless, it remains unclear whether the observed difference in Fig. 2 is due to different thermobarometers used (e.g., Xu X S et al., 1999; Xu Y G et al., 1999) and/or data quality, or truly reflect different thermal gradients for different localities.

These problems are elaborated in this article by applying the same pairs of thermometer and barometers on the data available for garnet-bearing peridotite, pyroxenite and granulite xenoliths from a number of localities in eastern China. This exercise is timely important because some new localities of garnet-bearing peridotite xenoliths (for which both reliable thermometer and barometer are available) are discovered in eastern China and also because increasing number of garnet peridotites and granulites are collected in recent years. On the other hand, the importance of garnet pyroxenites in the investigation of lithospheric geotherm has increasingly been recognized (Chen et al., 1996; Xu X S et al., 1996; Amundsen et al., 1987; O'Reilly and Griffin, 1985; Griffin et al., 1984). Given their common coexistence with spinel peridotites, garnet pyroxenites can yield information as to the thermal state for the lithospheric section occupied by spinel-facies peridotites, thus making it possible to overcome the aforementioned second problem associated with Xu Y G et al. (1995). The obtained data and inferred thermal state of the lithosphere will be evaluated in terms of major tectonic unites in eastern China (NE China, South China and North China) and major geological feature (e.g., north-south gravity lineament). These data, in combination with recent geophysical data, will be used to assess the nature of the stratigraphy and architecture of the lower crust and uppermantle beneath eastern China. We hope that this effort may provide a basic framework for the 4-D lithosphere mapping, one of key contents of the ongoing Cratonic Destruction Project in eastern China.

SAMPLE LOCALITIES AND DATA SCREEN

Xenoliths used in this study were collected from over twenty localities of Cenozoic basalts and/or mafic rocks/pipes in Northeast China, North China and South China (Fig. 2, Table 1). The locality in order from north to south include, Chao'erhe (Fan et al., 2008), Hannuoba (Chen et al., 2001; Shi et al., 2000), Nüshan (Xu X S et al., 1998), Xinchang (Lin et al., 1995; Xu Y G et al., 1995; Fan et al., 1989), Xilong (Yu et al., 2003), Mingxi (Lin et al., 1999a; Xu X S et al., 1998). The locality containing garnet pyroxenites include: Jiaohe (Yu, 2008), Kuandian (Fang and Ma, 1998), Hannuoba (Chen et al., 2001; Shi et al., 2000), Shanwang (Zheng et al., 2006), Nüshan (Huang et al., 2004; Xu X S et al., 1998), Qilin (Xu X S et al., 1996) and Leizhou (Huang et al., 2007; Lin et al., 2003; Yu et al., 2003). Granulite localities include Hannuoba (Chen et al., 2001; Huang et al., 2001), Nüshan (Huang et al., 2004) and Mingxi (Huang et al., unpublished data). These xenolith localities mostly occur to east of the DTGL. Specifically, Jiaohe is located in NE China, Nüshan, Shanwang and Kuandian in North China, and Leizhou Peninsula, Mingxi, Xinchang, Qilin in South China. Only two localities (Hannuoba, Chao'erhe) are situated to west of the DTGL (Fig. 2).

Mineral compositions are taken from literature (e.g., Fan et al., 2008; Huang et al., 2007, 2004, 2001; Zheng et al., 2006; Lin et al., 2003, 1999a, 1995; Yu et al., 2003; Chen et al., 2001; Fang and Ma, 1999; Xu X S et al., 1998, 1996; Xu Y G et al., 1998, 1993; Fan and Hooper, 1989). The data are screened before the calculation. Only electron microprobe (EPMA) data are used. The analyses with total less than 99% or greater than 101% are not used. Wet chemistry data collected in the eighties are not considered either. One of the most important pre-request for thermobarometric calculation is the thermal and compositional equilibrium between co-existing minerals. Because thermobarometry commonly involves Mg-Fe equilibrium between garnet and pyroxenes, we evaluate Mg-Fe partition between co-existing minerals for the purpose equilibrium assessment. There are excellent line correlations between $Mg^{\#}$ of orthopyroxene and clinopyroxene (Fig. 3a) and very well curve relations between $Mg^{\#}$ of garnet and those of orthopyroxene/clinopyroxene (Figs. 3b–3c), which strongly suggest that compositional equilibrium between co-existing minerals of garnet-bearing pyroxenites and peridotites

Table 1 *T-P* estimates for granulites, garnet-bearing pyroxenite and lherzolite xenoliths from eastern China

Sample	Rock*	*T* (℃)	*P* (10^{-1} MPa)	Data sources
Qilin				
Q9307	I	904	11.7	Xu X S et al. (1996)
Q9323	I	904	11.7	Xu X S et al. (1996)
Q9324	I	904	11.7	Xu X S et al. (1996)
Q8907	II	957	13.5	Xu X S et al. (1996)
Q9352	I	941	12.2	Xu X S et al. (1996)
Q9353	I	935	10.1	Xu X S et al. (1996)
Q9355	I	914	12	Xu X S et al. (1996)
Q9327	I	939	11.9	Xu X S et al. (1996)
Q9351	I	941	13.9	Xu X S et al. (1996)
QL1	I	891	11.2	Xu X S et al. (1996)
QL8	I	860	10.1	Xu X S et al. (1996)
QL13	I	839	6.9	Xu X S et al. (1996)
QL21	I	847	9.3	Xu X S et al. (1996)
Mingxi				
DYK-1	III	1 156	21.9	Lin et al. (1999)
DYK-2	III	1 100	21	Lin et al. (1999)
DYK-3	III	1 170	22.4	Lin et al. (1999)
DYK-6	III	1 108	20	Lin et al. (1999)
DYK-7	III	1 106	21.4	Lin et al. (1999)
DYK-8	IV	1 091	20.9	Lin et al. (1999)
DYK-16	IV	1 171	23	Lin et al. (1999)
DYK-21	IV	1 144	21.4	Lin et al. (1999)
DYK-23	III	1 071	19.7	Lin et al. (1999)
DYK-29	IV	1 097	20.6	Lin et al. (1999)
DYK-30	III	1 065	19.5	Lin et al. (1999)
DYK-36	IV	1 061	19.6	Lin et al. (1999)
DYK-41	III	1 159	21.9	Lin et al. (1999)
DYK-42	IV	1 126	21.7	Lin et al. (1999)
DYK-43	IV	1 133	22	Lin et al. (1999)
DYK-44	IV	1 087	19.9	Lin et al. (1999)
DYK-45	IV	1 158	22.1	Lin et al. (1999)
MX07-1	V	713	6.6	Unpublished data
MX09-2	V	663	6.4	Unpublished data
MX09-4	V	631	4.6	Unpublished data
MX09-6	V	715	6.3	Unpublished data
Leizhou Peninsula				
XW-3NJ	I	915	12.1	Yu et al. (2003)
XW-3	I	994	15.3	Yu et al. (2003)
LZ-51	II	1 072	19.4	Yu et al. (2003)
LZ-47-2	I	1 007	15.1	Yu et al. (2003)
LZ-47-1	I	1 017	15.7	Yu et al. (2003)
LZ-46	I	961	15	Yu et al. (2003)
LZ-44-IV	II	1 031	17.6	Yu et al. (2003)
LZ-44-III	II	1 023	16.5	Yu et al. (2003)
LZ-44-II	II	1 028	18.5	Yu et al. (2003)
LZ-44-I	II	1 035	18.6	Yu et al. (2003)
LZ-42	II	1 109	24.3	Yu et al. (2003)
LZ-37	II	1 034	18.2	Yu et al. (2003)
LZ-30	II	969	16	Yu et al. (2003)
LZ-34	II	1 042	18.9	Yu et al. (2003)
LZ-15	II	963	14.5	Yu et al. (2003)
gyx-35	II	1 017	18.3	Lin et al. (2003)
gyx-29	II	941	13.7	Lin et al. (2003)
gyx-29LB	II	901	12.3	Huang et al. (2007)
gyx-29LA	II	901	12.2	Huang et al. (2007)
gyx-29GA	II	897	11.9	Huang et al. (2007)
Xinchang				
ZN-20	IV	1 215	23.4	Fan and Hooper (1989)
ZN-12	IV	1 171	21.2	Fan and Hooper (1989)
ZN-8	IV	1 177	23.7	Fan and Hooper (1989)
XC-14	IV	1 153	18.8	Lin et al. (1995)
XC-8	IV	1 190	22.2	Lin et al. (1995)
XC-1	IV	1 189	22.7	Lin et al. (1995)
Xilong				
XL-1-1	V	786	9.9	Yu et al. (2003)
XL-1-2	V	801	10.2	Yu et al. (2003)
Anyuan				
S-10(2)	IV	1 182	23.9	Zheng et al. (2004)
Nüshan				
Nu9408-2	I	950	14.5	Xu X S et al. (1998)
Nu9408-1	I	924	13.4	Xu X S et al. (1998)
NSGP1	I	926	13.5	Xu X S et al. (1998)
NS93-4V	II	1 163	20.6	Xu X S et al. (1998)
Nu9503	II	1 172	20.5	Xu X S et al. (1998)
Nu1993-2	II	1 148	19.9	Xu X S et al. (1998)
Nu1993	II	1 154	19.9	Xu X S et al. (1998)
NS9313	II	1 165	20.2	Xu X S et al. (1998)
Nu9621	III	1 129	17.9	Xu X S et al. (1998)
Nu9604	III	1 127	18.3	Xu X S et al. (1998)
NS9313-3	III	1 167	19.1	Xu X S et al. (1998)
NS9313-2	III	1 153	18.7	Xu X S et al. (1998)
Nu1989	III	1 122	19.4	Xu X S et al. (1998)
Nu9413	III	1 147	19.1	Xu X S et al. (1998)
Nu9301-2	III	1 153	18.7	Xu X S et al. (1998)
Nu9414	III	1 116	21.1	Xu X S et al. (1998)
Nu9410	III	1 163	21.9	Xu X S et al. (1998)
Nu9407	IV	1 159	22.4	Xu X S et al. (1998)
Nu9506	IV	1 161	19.2	Xu X S et al. (1998)
Nu9504	IV	1 154	18.8	Xu X S et al. (1998)
Nu9502	IV	1 174	19.5	Xu X S et al. (1998)
NS218	IV	898	13.1	Unpublished data
N-3	III	1 163	19.1	Jin and Pan (1998)
NS201	V	793	8.2	Huang et al. (2004)

Continued

Sample	Rock*	T (℃)	P (10^{-1} MPa)	Data sources
NS202c	V	765	7.9	Huang et al. (2004)
NS202r	V	790	8.2	Huang et al. (2004)
NS203	V	749	6.1	Huang et al. (2004)
NS204	V	719	7.4	Huang et al. (2004)
NS205	V	786	6.9	Huang et al. (2004)
NS206	V	792	8.5	Huang et al. (2004)
NS207	V	745	6.8	Huang et al. (2004)
NS210	V	656	5.2	Huang et al. (2004)
NS212	V	731	6.9	Huang et al. (2004)
NS213	V	758	5.9	Huang et al. (2004)
NS214	V	672	3.9	Huang et al. (2004)
Nu8901	V	708	4.2	Xu X S et al. (1998)
Nu8902	V	778	6.7	Xu X S et al. (1998)
Nu8903	V	699	3.4	Xu X S et al. (1998)
Nu9518	V	716	6.4	Xu X S et al. (1998)
Nu9521	V	730	6.3	Xu X S et al. (1998)
Nu9523	V	744	5.5	Xu X S et al. (1998)
Hannuoba				
90DA11	II	1 114	23	Chen et al. (2001)
JSB	II	1 065	19	Chen et al. (2001)
95SQ9	II	1 062	18.8	Chen et al. (2001)
95JSB4	II	1 090	20	Chen et al. (2001)
30J27	II	1 089	19.8	Chen et al. (2001)
TGZ	II	1 098	19.1	Chen et al. (2001)
T253	II	1 127	20.4	Chen et al. (2001)
NT26	I	1 216	23.9	Chen et al. (2001)
30J26	II	1 088	20.1	Chen et al. (2001)
2XM2	I	1 082	19.7	Chen et al. (2001)
Dmp-9	VI	783	7.79	Chen et al. (2001)
Dmp-7	VI	771	9.07	Chen et al. (2001)
Dmp-4	VI	798	7.7	Chen et al. (2001)
DM3	V	805	8.8	Chen et al. (2001)
95SQ1	V	832	10.4	Chen et al. (2001)
95DA15	V	834	9.4	Chen et al. (2001)
93DA8	V	816	9.3	Chen et al. (2001)
90DA9	V	775	9.5	Chen et al. (2001)
90DA4	V	828	9.4	Chen et al. (2001)
D39	V	794	9.4	Unpublished data
D36	V	609	7.2	Unpublished data
D34	V	729	9.5	Unpublished data
D22	V	739	8	Unpublished data
Hebi				
Hebi-1	III	1 167	18.9	Fan et al. (2008)
Kuandian				
96Kd15	II	1 059	17	Fang and Ma (1999)
96Kd12	I	1 009	17.4	Fang and Ma (1999)
96Kd11	II	1 042	16.9	Fang and Ma (1999)
96Kd03	II	1 027	18.6	Fang and Ma (1999)
95Kd24	I	1 044	16.2	Fang and Ma (1999)
95Kd11	I	1 031	15.6	Fang and Ma (1999)
96Kd17	I	1 074	17.8	Fang and Ma (1999)
95Kd03	I	1 070	16.9	Fang and Ma (1999)
Shanwang				
SW04-6	III	1 174	19.7	Zheng et al. (2006)
SW04-2	III	1 090	16.3	Zheng et al. (2006)
SW01-8	IV	1 182	24.2	Zheng et al. (2006)
SW01-1	IV	1 164	22.8	Zheng et al. (2006)
SW0193	III	1 007	17.2	Zheng et al. (2006)
SW0169	III	1 100	19.9	Zheng et al. (2006)
Jiaohe				
YQSX-13	II	1 006	16.5	Yu (2008)
YQS-19	I	825	10.2	Yu (2008)
YQS-18	I	904	13.9	Yu (2008)
YQSX-4	II	948	15.6	Yu (2008)
YQSX-12	II	901	13.4	Yu (2008)
YQSX-7	I	1 024	16.1	Yu (2008)
YQSX-2	I	1 030	17.5	Yu (2008)
BSK-12	I	989	16.6	Yu (2008)
BSK-13	II	1 001	16.5	Yu (2008)
Chao'erhe				
07WNP11	IV	1 311	28.9	Fan et al. (2008)
07WNP09	IV	1 326	26	Fan et al. (2008)
07WNP07	IV	1 227	27.6	Fan et al. (2008)
07WNP06	IV	1 155	23.2	Fan et al. (2008)
07WNP05	IV	1 337	30.3	Fan et al. (2008)
07WNP04	IV	1 143	24.3	Fan et al. (2008)
07WNP02	IV	1 192	27.6	Fan et al. (2008)
07DHL02	IV	1 198	26.7	Fan et al. (2008)
07DHL01	IV	1 121	23.1	Fan et al. (2008)
Chaoerhe1	IV	1 192	27.5	Fan et al. (2008)
Lixian (Western Qinling)				
XQL-1	IV	1 124	23.1	Yu et al. (2001)
XQL-2	IV	1 191	24.1	Yu et al. (2001)
XQL-3	II	1 263	33.6	Yu et al. (2001)
XQL-4	II	1 217	30.4	Yu et al. (2001)
XQL-5	III	1 147	23.8	Su et al. (2007)

* Rock types and *T-P* methods: (I) spinel-garnet pyroxenite, T_{BK2P}/P_{NG}; (II) garnet pyroxenite, T_{BK2P}/P_{NG}; (III) spinel-garnet lherzolite, T_{BK2P}/P_{BKN}; (IV) garnet lherzolite, T_{BK2P}/P_{BKN}; (V) garnet-bearing granulite, T_{BK2P}/P_{NG}; (VI) garnet-free granulite, T_{BK2P}/P_{PM}.

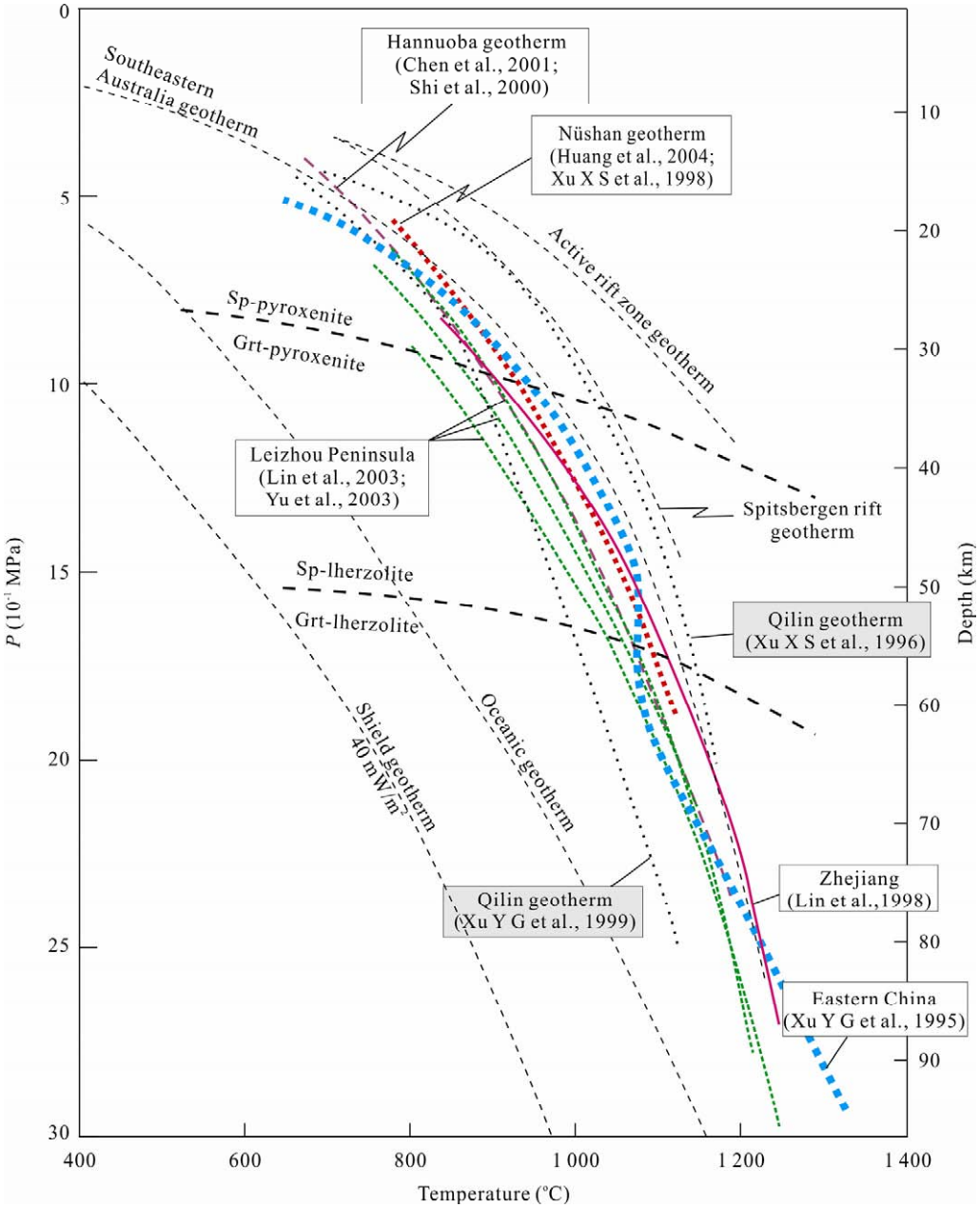

Figure 2. The existing geotherms constructed on the basis of equilibrium pressures and temperatures of xenoliths from eastern China. Data source: Xu Y G et al. (1999, 1995); Xu X S et al. (1998, 1996); Chen et al. (2001); Lin et al. (2003, 1998); Huang et al. (2004) and Yu et al. (2003). The comparative geotherms (shield, oceanic, Spitsbergen RIFT and southeastern Australia) are after O'Reilly and Griffin (1996). The transition between spinel- and garnet-lherzolites is from O'Neill (1981), and the spinel pyroxenite-garnet pyroxenite boundary is from Herzberg (1978).

is attained for the xenoliths selected for this study.

SELECTION OF GEOTHERMOBAROMETERS IN TERMS OF MULTIPLE CRITERIA

A large number of thermometer and barometer are available in literature. Different thermobarometers are calibrated for different purposes and using different criteria. It is therefore of ultimate importance to choose appropriate thermobarometer(s) for the purpose of construction of thermal gradient for a given lithosphere. The criteria used in evaluating the reliability of a given thermometer or barometer is reiterated here (Xu Y G et al., 1999; Xu Y G, 1993): (1) A reliable thermobarometric calibration should perfectly

reproduce the experimentally reversed data in natural systems under high temperature and pressure (Brey and Köhler, 1990; Carswell and Gibb, 1987; Bertrand and Mercier, 1985); (2) estimated *P-T* values should be consistent with known phase relationships (Finnerty and Boyd, 1984; Griffin et al., 1984); and (3) applications of geothermobarometric data to composite xenoliths should yield similar estimates for different parts of the composites. Another approach but more rarely used is to directly determine the stability limits of mineral assemblage by experiments on individual xenoliths (Adam et al., 1992; Irving, 1974).

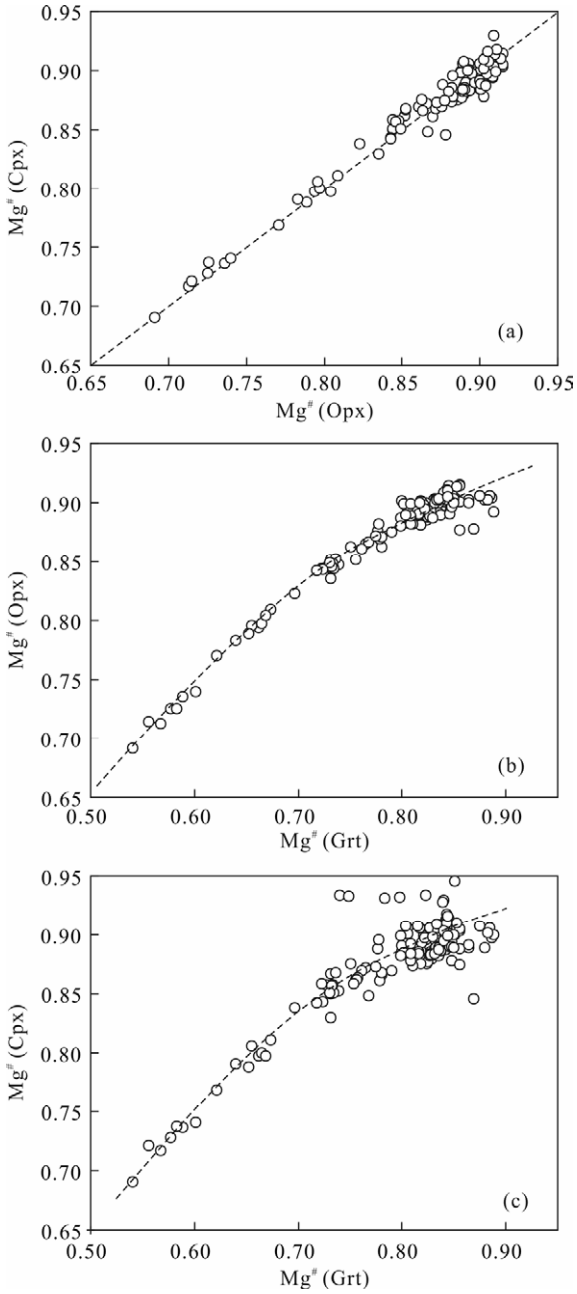

Figure 3. Partitioning of Fe-Mg between co-existing garnet, clinopyroxene and orthopyroxene for peridotite and pyroxenite xenoliths selected for this study. Data from Xu X S et al. (1998, 1996), Lin et al. (1999, 1995), Fang and Ma (1999), Yu et al. (2003), Fan et al. (2008, 1989), Jin and Pan (1998), Chen et al. (2001), Yu (2001), Zheng et al. (2006, 2001), Huang et al. (2007, 2004), Su et al. (2007), Yu (2008).

The first criterion has been used by Bertrand and Mercier (1985) and Carswell and Gibb (1987) in the formulation of new geothermobarometers and the evaluation of existing ones. It has been shown that this may be the most reasonable approach in any thermobarometric evaluation (e.g., Brey and Köhler, 1990). From Figs. 4a and 4c it is apparent that the BM thermometer (Bertrand and Mercier, 1985) nicely fits the experimental temperatures, whereas the Ellis and Green (1979) thermometer underestimates the experimental temperatures for temperatures >1 200 ℃ and overestimates for temperatures <1 200 ℃ (Fig. 4c). When applied to the experimentally crystallized garnets and pyroxenes, the Ellis and Green (1979) calibration is found to systematically overestimate the temperature by about 150 ℃ for the pressure range of garnet pyroxenites (Green and Adam, 1991). A similar remark was also made by Ai (1994) who has accordingly revised the Fe-Mg exchange thermometer based on a comprehensive data set of both ultramafic and mafic compositions. The Sachtleben and Seck (1981) thermometer slightly underestimates the experimental temperatures for temperatures <1 100 ℃ but the discrepancy becomes important for temperatures >1 100 ℃ (Fig. 4d). Accordingly, this empirical thermometer has been improved by Witt-Eickschen and Seck (1991).

Figure 5 shows the results for barometers. Similar to the conclusion of Carswell and Gibb (1987), it is clear that the barometer of Wood (1974) underestimates the experimental pressures. By contrast, the barometer of Nickel and Green (1985) reasonably reproduces the experimental pressures.

Three phase relationships have been used so far in thermobarometric evaluations: (1) graphite-diamond transition (Finnerty and Boyd, 1984); (2) spinel to garnet pyroxenite transition (Griffin et al., 1984); and (3) spinel to garnet lherzolite transition

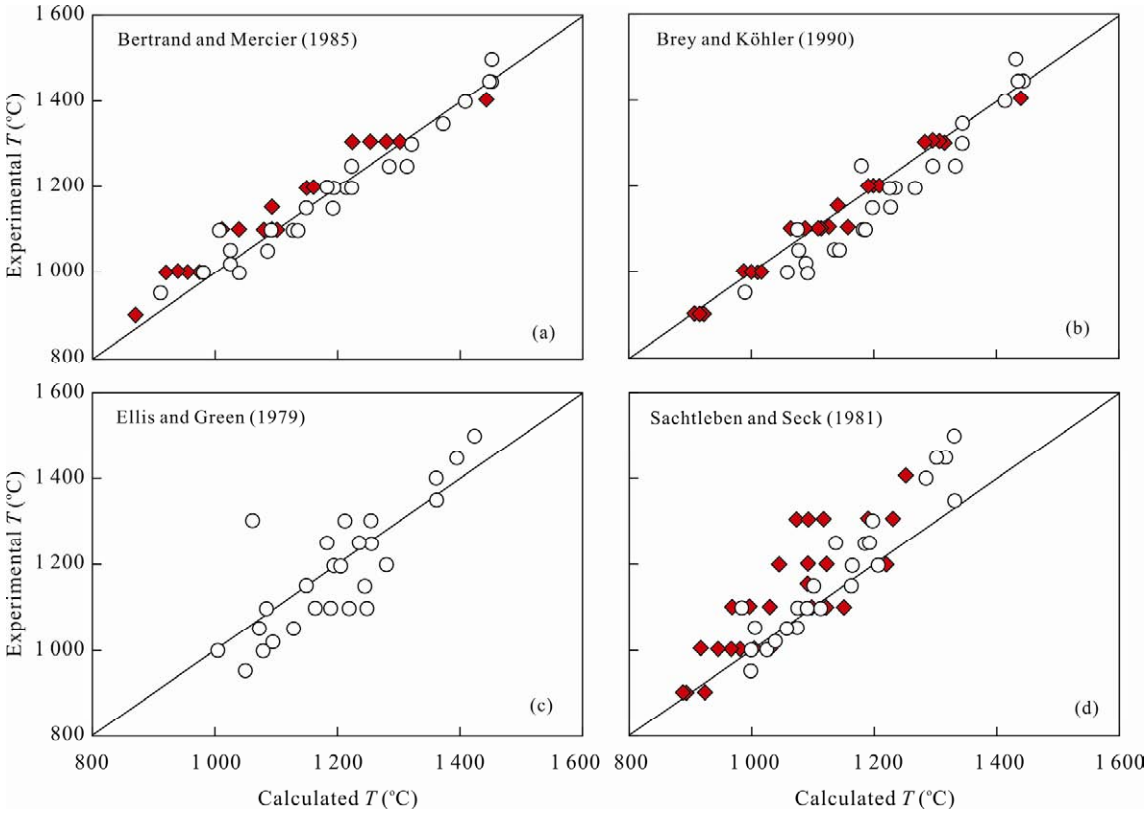

Figure 4. Comparison between the calculated temperatures from different thermometers and experimental temperatures (after Xu Y G et al., 1999). (a) Bertrand and Mercier (1985); (b) Brey and Köhler (1990), (c) Ellis and Green (1979); and (d) Sachtleben and Seck (1981). Filled diamond: data from Brey and Köhler (1990); open circle: data from Akella (1976), Mori and Green (1978).

(O'Reilly and Griffin, 1985). We performed a test for two pairs of thermometers/barometers listed above to see (1) whether they are consistent with the graphite-diamond reaction using the available data on graphite- and diamond-bearing xenoliths (Zheng et al., 2006; Pearson et al., 1994; Jaques et al., 1990; Shee et al., 1982; Pokhilenko et al., 1977; Dawson and Smith, 1975; Nixon and Boyd, 1973), as well as multiphase inclusions in diamond (Tsai et al., 1979); (2) whether they are consistent with the spinel-garnet transitions using mineral chemistry data on garnet-bearing xenoliths (including pyroxenites and peridotites) from eastern China. It is clear from Figs. 4–5 that the BK2P/NG method (Brey and Köhler (1990)/Nickel and Green (1985)) yields results consistent with both the graphite-diamond transition of Kennedy and Kennedy (1976) and the spinel-garnet transition, whereas the estimates of the EG/W method are only consistent with the spinel-garnet transition but not with the graphite-diamond reaction (Xu Y G et al., 1999). These results strongly suggest that the BK2P/NG (as well as the T_{BK2P}/P_{BKN} method (Brey and Köhler (1990)/Brey and Köhler (1990)) which yields comparable results) is the first choice when estimating *P-T* of Mg-rich rocks.

The third criterion is largely based on equilibrium composite xenoliths. The different parts of a composite are located at the same depths, therefore application of a geothermometer should yield similar temperature estimates for different parts of the xenoliths. However, this approach is frequently hampered because the lherzolite part in composites could be thermally affected by the magmatic intrusion represented by the pyroxenite vein (Xu X S et al., 1999).

The methods mentioned above are only associated with garnet-bearing xenoliths. For the *P-T* estimation for garnet-free granulites, McCarthy and Patiño Douce (1998)'s empirical geobarometer and Brey and Köhler (1990)'s two-pyroxene thermometer are used. The reasoning for this choice is provided by Huang et al. (2004).

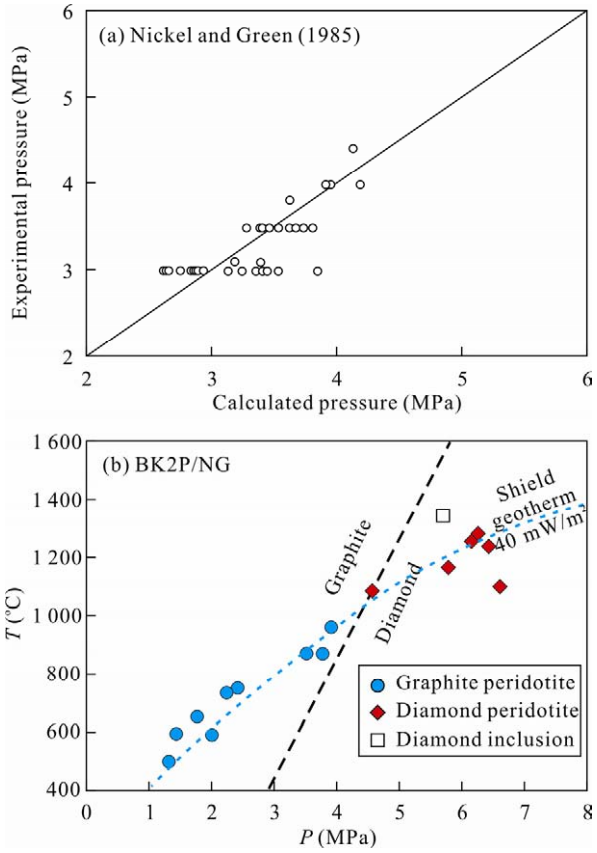

Figure 5. (a) Comparison between the calculated pressures of Nickel and Green (1985)'s barometer and experimental pressures. Data source is the same as in Fig. 4; (b) comparison between *P-T* calculated by BK2P/NG and the graphite-diamond transition. Data of graphite- and diamond-bearing peridotites and coexisting multiphase inclusions in diamond are after Zheng et al. (2006), Pearson et al. (1994), Jaques et al. (1990), Shee et al. (1982), Tsai et al. (1979), Pokhilenko et al. (1977), Dawson and Smith (1975), and Nixon and Boyd (1973). The graphite-diamond transition is taken from Kennedy and Kennedy (1976).

RESULTS

A summary of estimated equilibrium temperatures and pressures are presented in Table 1, and results are plotted in Fig. 6. The majority of calculation results are consistent with experimental phase relationship. Specifically, the equilibrium *P-T* places garnet pyroxenites within the stability field of garnet-facies pyroxenite (O'Neill, 1981), and garnet peridotites within the stability field of garnet peridotite (Fig. 6). These demonstrate the robustness of the calculation results. Below, the results are described in terms of different tectonic units in eastern China, namely North China craton, northeastern China and South China.

North China Craton

The typical xenolith locality in eastern North China craton (NCC) is Nüshan, where xenoliths include garnet and spinel peridotites, garnet pyroxenites and granulites covering a full range of the lithosphere (Huang et al., 2004; Xu X S et al., 1998). The estimated *P* and *T* values for the Nüshan xenoliths range from 0.4 to 2.4 MPa and from 600 to 1 200 ℃, thus defining tightly a geotherm. Data for garnet pyroxenites from Kuandian and garnet peridotites from Shanwang are also plotted proximal to this geotherm (Fig. 6a), suggesting that the Nüshan geotherm represent that for the lithosphere under the eastern NCC. This geotherm corresponds to a high thermal gradient (~ 80 mW/m^2). It is noted that the geotherm is composed of two sections: the section with pressure less than 2 MPa is characterized by a slow slope, whereas the section with pressure greater than 2 MPa shows a roughly vertical pattern. Likely, the xenoliths from eastern NCC record two different mechanisms of heat transfer between lithosphere and asthenosphere (see DISCUSSION).

Thermal state for the lithosphere under western NCC is constrained by the xenoliths from Hannuoba. *P-T* data are restricted to granulites and garnet pyroxenites and fall into two groups (<1.1 and >1.5 MPa). Equilibrium *P* and *T* between them are not observed. These data nevertheless define a geotherm corresponding to ~70 mW/m^2 (Fig. 6b). This thermal gradient, slightly lower than that for eastern NCC, is characterized by a uniform slope, implying a single heat transfer mechanism for the lithosphere sampled by the Hannuoba xenoliths.

Northeastern China

Only two localities (Jiaohe and Chao'erhe) in northeastern China contain garnet-bearing xenoliths. In addition, the number of samples from these two localities is relatively small, making the geotherm for this region poorly constrained. The estimated *P* and *T* for garnet pyroxenites from Jiaohe vary from 0.8 to 1.8 MPa and from 820 to 1 030 ℃, respectively. They

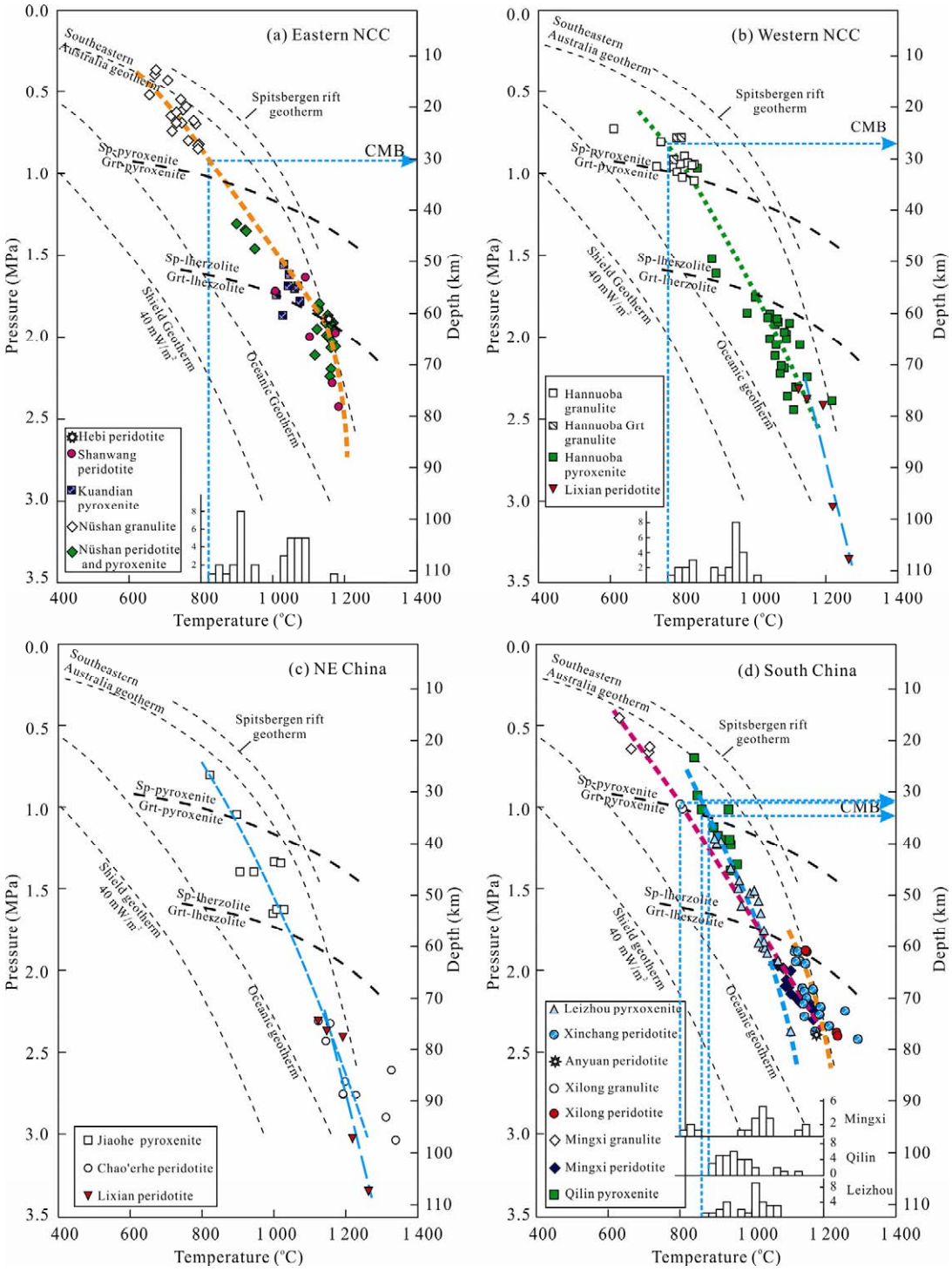

Figure 6. Equilibrium pressures and temperatures calculated for screened xenoliths from eastern China. (a) Eastern North China craton (NCC); (b) western NCC; (c) northeastern (NE) China; (d) South China. Data source: Chao'erhe (Fan et al., 2008), Hannuoba (Chen et al., 2001; Shi et al., 2000), Nüshan (Huang et al., 2004; Xu X S et al., 1998), Xinchang (Lin et al., 1995; Xu Y G et al., 1995; Fan and Hooper, 1989), Mingxi (Lin et al., 1999; Huang et al., unpublished data), Jiaohe (Yu, 2008), Kuandian (Fang and Ma, 1999), Shanwang (Zheng et al., 2006), Qilin (Xu X S et al., 1996), Leizhou (Huang et al., 2007; Lin et al., 2003; Yu et al., 2003), Lixian (Su et al., 2007; Yu et al., 2001), Anyuan (Zheng et al., 2004), Hebi (Fan et al., 2008). The comparative geotherms (shield, oceanic, Spitsbergen rift and southeastern Australia) are after O'Reilly and Griffin (1996). The transition between spinel- and garnet-lherzolites is from O'Neill (1981), and the spinel pyroxenite-garnet pyroxenite boundary is from Herzberg (1978).

thus only provide thermal gradient for the uppermost upper mantle under the region to east of DTGL in NE China. The estimated *P* and *T* for garnet pyroxenites from Chao'erhe vary from 2.4 to 3 MPa and 1 120 to 1 340 ℃, respectively. The estimated pressures are considerably higher than those obtained for garnet peridotites from the NCC, but are similar to those for Qinling peridotites (Yu et al., 2001). It is noted that the thermal gradient defined by the Jiaohe xenoliths resembles the Nüshan geotherm, and equilibrium *P-T* data for the Chao'erhe xenoliths are plotted along the extended trend of the Hannuoba geotherm. This indicates the contrasting thermal gradient for the lithosphere across the DTGL.

South China

P-T data for the xenoliths from South China (Fig. 6c) do not define a single slope. Notably, the data for the Qilin xenoliths define a slope which is different from that for the Mingxi xenoliths. It is possible that the Mingxi and Xinchang xenoliths form one gradient with a kink at about 2 MPa. However, the slower slope for the deep lithosphere compared to shallow section is inconsistent with the heat transfer between lithosphere and asthenosphere (McKenzie and Bickle, 1988). Consequently, we believe that the Mingxi and Qilin xenoliths define two different thermal gradients. This is further supported by the Mingxi granulites whose equilibrium pressures and temperatures are distributed along the extended trend defined by Mingxi garnet peridotites (Fig. 6d). In spite of small number, the Xinchang samples seem to form a further different gradient.

DISCUSSION

Two Types of Geotherm for the Lithosphere beneath Eastern China

The data presented in this study apparently reveal two types of geotherm for the lithosphere beneath eastern China (Fig. 7). The first type, as exampled by the geotherms of Hannuoba, Mingxi and probably NE China, is characterized by constant slope of data in the *P-T* space (Fig. 7a). Noticeably, thermal gradients for three different regions are very similar. The second type, as exampled by the geotherms of Nüshan and probably Xinchang, is characterized by variable slopes in the *P-T* space (Fig. 7b). Specifically, the samples with pressure <2 MPa define a slow slope, whereas the samples with pressure >2 MPa define a virtually vertical slope. The following considerations make us believe that the two types of thermal gradient are real, rather than an artifact of thermobarometric calculation.

(a) The different slopes in the second type of geotherm may correspond to different heat transfer mechanisms, with conductive transfer for the shallow upper mantle and advective transfer for the deep mantle. This observed transition in thermal transfer mechanism is essentially similar to that predicted by theoretical modeling (McKenzie and Bickle, 1988), and the transition zone may correspond to the thermal boundary layer (TBL). We thus propose that the samples defining such a kind of geotherm must have been derived from all the range of the lithosphere and the samples with the highest *P* and *T* provide maximum estimates on the thickness of the lithosphere at the given region. Following this line of reasoning, the thickness of the lithosphere beneath eastern NCC is about 70 km, in good agreement with the recent seismic results (Chen et al., 2009).

(b) The higher thermal gradient for eastern NCC is consistent with higher equilibrium temperatures for spinel peridotites collected from this region, compared to those for other areas. For example, equilibrium temperatures for spinel peridotites from eastern NCC range from 800–1 200 ℃, with two peaks at 900 and 1 050 ℃. There are a significant number of samples with temperature of 1 000–1 100 ℃ in eastern NCC. In the regions (western NCC, NE China) characterized by the first type of geotherm, the equilibrium temperatures are relatively low, mostly concentrated between 800–1 000 ℃, despite a few >1 000 ℃ (Fig. 8). If these spinel peridotites are equilibrated within the spinel facies stability, i.e., under same pressure range, it can be inferred that higher temperatures are indicative of a higher geotherm.

(c) As will be discussed in the following sections, the higher thermal gradient is, the thinner lithosphere is. In the case of eastern NCC, the lithosphere is inferred to be ~70 km thick. Given the experimental determined spinel-garnet phase transition at 70–80 km (Robinson and Wood, 1998), lithospheric xenoliths

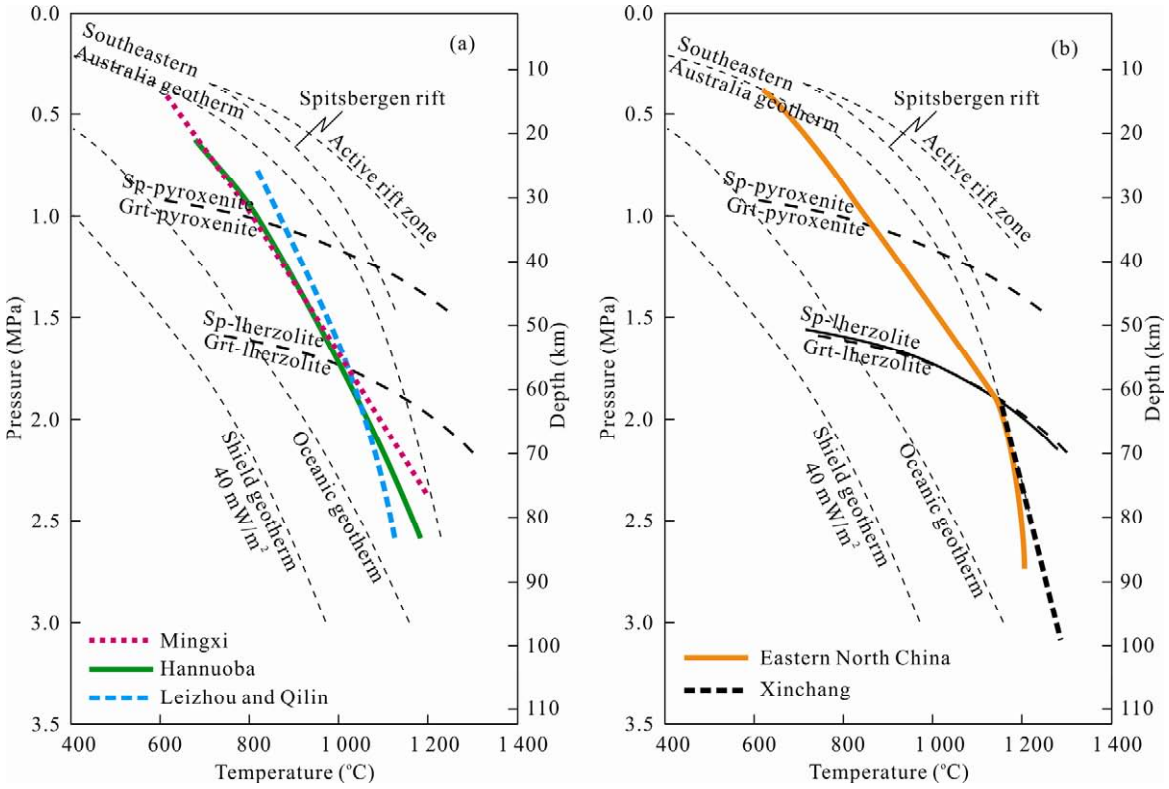

Figure 7. Two types of xenolith-derived geotherms in eastern China.

sampled by asthenosphere-derived melts will be essentially spinel-facies peridotites. The same reasoning leads to the suggestion that both spinel and garnet facies peridotites can be found in the regions with low thermal gradient, because the depth to the lithosphere-asthenosphere boundary in these areas is >90–100 km, well below the depth at which spinel-garnet phase transition occurs. This prediction is matched by observation that so far garnet peridotites are exclusively found in the areas with low thermal gradient (west of the DTGL, South China), whereas so far no garnet peridotite xenoliths are observed in eastern NCC (high thermal gradient).

The two types of geotherm are not mutually exclusive. The second type may represent a geotherm for whole lithospheric section including both mechanical boundary layer (MBL) and TBL, while the first type may only depict the MBL. In particular, the peculiar geotherm for Xinchang may only depict the TBL. The reason why different types of geotherm, or different sectors are sampled by xenoliths remains unclear. It may be related to entrainment mechanism of xenoliths by basalts, a phenomenon not well understood so far.

It should be noted the peculiarity of the geotherm for Qilin and Leizhou, which crosses the first type of geotherm. It is also characterized by a weak convex-upward pattern, probably reflecting a transitional feature between conductive and advective heat transfer. Qilin and Leizhou are situated to the northern margin of South China Sea, an area intruded by upwelled seismically low velocity materials (Lei et al., 2009). It is therefore possible that the thermal perturbation associated with Qilin and Leizhou may reflect the effect of impregnation of mantle plume on the base of the lithosphere.

Heterogeneous Lithospheric Structure in Eastern China

Thermal gradient, in comparison with equilibrium temperature of spinel peridotites and seismic data, can be used to characterize the nature of the crust-mantle boundary (CMB) and the lithosphere-asthenosphere boundary (LAB) for a given region. The information as to these important boundaries is pivotal to understanding deep lithospheric processes and magma genesis.

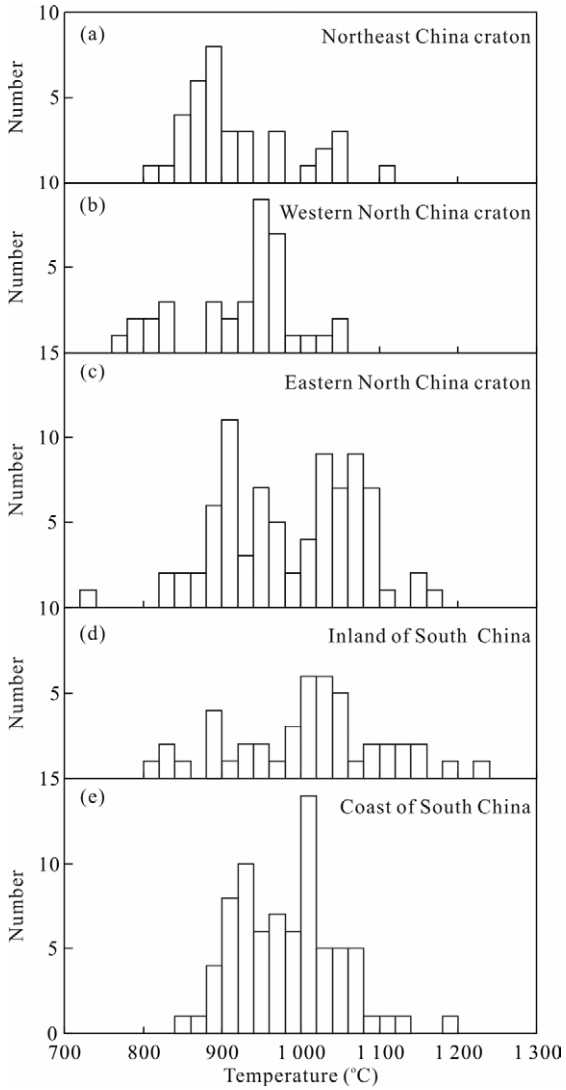

Figure 8. Histograms of equilibrium temperatures for spinel peridotites from different regions in eastern China. Northeast China: Wangqing (Xu Y G et al., 1998) and Huinan (Xu Y G et al., 2003). Western NCC: Hannuoba (Chen et al., 2001; Shi et al., 2000) and Datong (Chen et al., 1997). Eastern NCC: Nüshan (Xu X S et al., 1998; Qi et al., 1995), Kuandian (Fang and Ma, 1998), Shanwang (Zheng et al., 1998), Hebi (Zheng et al., 2001) and Pangshishan (Liu and Yan, 2007; Chen et al., 1994). Inland South China: Mingxi (Lin et al., 1999; Qi et al., 1995), Anyuan (Zheng et al., 2004). Coast of South China: Xinchang (Lin et al., 1995; Xu Y G et al., 1995; Fan and Hooper, 1989), Qilin (Xu X S et al., 1996; Qi et al., 1995) and Leizhou (Yu et al., 2003).

Depth to Moho

The "seismic Moho" is defined as the base of the crust, across which the compressional wave velocity increases rapidly to ~8 km/s, whereas the crust-mantle boundary (CMB) is the transition between felsic-mafic crustal rocks and a dominantly ultramafic upper mantle (Griffin and O'Reilly, 1987). They are not always consistent, particularly in continental regions of high heat flow where the seismic Moho may lie deeper than the CMB (Griffin and O'Reilly, 1987). The depth to CMB can be estimated by comparing the lowest temperature estimates of the spinel lherzolites and xenolith-based geotherm (O'Reilly and Griffin, 1985). If the relative proportion of mantle xenoliths at the earth surface can be taken as indicative of the lithology of the upper mantle, then spinel peridotite is the dominant rock of the shallow mantle. It is thus reasonable to infer that the shallowest depth from which spinel peridotites were sampled by the host basalts defines the maximum thickness of the crust. If the depth to CMB is greater than the seismic Moho, a crust-mantle transition zone can be inferred (O'Reilly and Griffin, 1996), probably indicative of magmatic underplating which took place previously. To investigate the depth to CMB, we compare histograms of equilibrium temperature with geotherm for the NCC, coast of South China and inland of South China, respectively.

North China

In eastern NCC, the equilibrium temperatures for the granulite xenoliths are all below 800 ℃, whereas mantle-derived xenoliths are mostly equilibrated at temperatures higher than 820 ℃ (Figs. 6a, 7). 820 ℃ is therefore considered as the temperature at the base of the lower crust. By reference of the geotherm in this area, this suggests that the depth to the CMB is ca. 30 km, consistent with the depth to Moho as revealed by seismic refraction data (Chen, 1988). In contrast, the depth to the CMB at Hannuoba (~28 km) is significantly shallower than the seismic Moho (~42 km, Table 2), implying a thick (~14 km) crust-mantle transition zone. The different crust-mantle structures in the NCC may have resulted from different degrees of magma underplating in the western and eastern NCC (Xu Y G, 2007; Huang et al., 2004). Magmatic underplating must have been important in western NCC, because geochronologic studies (Wilde et al.,

2003; Fan et al., 1998) reveal that magma underplating occurred during the Late Mesozoic, coeval with the initiation of widespread thermo-tectonic reactivation of the NCC (Xu Y G, 2001; Griffin et al., 1998). In contrast, underplating was minor in eastern NCC given the pre-dominant "Proterozoic age" of the granulite xenoliths and the coincidence of the "petrologic" and "seismic" Mohos (Huang et al., 2004). Alternatively, the contrast in crust structures in the regions separated by the DTGL may be related to crustal foundering processes (Gao et al., 2004; Xu Y G, 2002).

Inland of South China (Mingxi)

Comparison of the lowest equilibrium temperatures of spinel peridotites from Mingxi yields the depth to the CMB for these areas is ca. 32 km (Fig. 6d). This estimate is close to the seismic Moho (Wang et al., 1993; Table 2). The consistency between the petrologic Moho and seismic Moho suggests an insignificant crust-mantle transition zone in this area. However, care should be taken because the equilibrium distribution pattern is irregular (Fig. 6d). Notably, there lack samples with temperature of 850–1 000 ℃, suggesting biased sampling of the lithospheric mantle by host rocks.

Coast of South China (Leizhou and Qilin)

Comparison of the lowest equilibrium temperatures of spinel peridotites from Leizhou and Qilin yields the depth to the CMB for these areas is ca. 31 and 35 km, respectively (Fig. 6d). These estimates are greater than the seismic Moho (28, 31 km) (Yao et al., 2006; Table 2). We don't know whether this contradiction is related to the error associated with thermobarometry and seismic investigation or to the representativeness of xenolith population. As noted above, the geotherm in this area is peculiar, probably reflecting heating of the lithosphere by impregnating plume. Alternatively, the anomalously high geotherm at the crust-mantle boundary may be related to lateral heat transport from the underplating materials in South China basin, where the seismic velocity structure (V_P=6.6–7.6 km/s) is suggestive of a thick crust-mantle transition zone.

Depth to LAB

According to McKenzie and Bickle (1988), the lithosphere includes TBL and overlying MBL. With the MBL, heat transport is via conduction, whereas in the TBL, both conduction and advection play role in heat transport. Compared to the MBL, the TBL is characterized by a steeper slope in the *P-T* space. The depth the transition between MBL and TBL provides an estimate to the lithospheric thickness. For the region where no MBL-TBL transition is observed, the greatest depth of garnet peridotites represents the minimum thickness of brittle lithosphere (O'Reilly and Griffin, 1996). Given the lack of evidence of a mantle plume for eastern China, potential temperature of the asthenosphere (T_P=1 280 ℃) (McKenzie and Bickle, 1988) is taken to reflect the maximum temperature at the base of the lithosphere. Projecting this temperature along a given geotherm yields a maximum estimation for the depth to the LAB. This is a reasonable assumption because the highest temperatures for spinel- and garnet-peridotites (1 150 to 1 200 ℃, 1 200 to 1 280 ℃, respectively; Table 1; Fig. 8) approach T_P (1 280 ℃).

Using this approach, the depth to LAB in eastern NCC is ca. 70 km, in remarkably good agreement with recent seismic investigation results (Chen, 1988; Table 2). In western NCC, the lithospheric thickness is greater than 90–100 km, again revealing the contrasting lithospheric structure across the DTGL. The thickness of the lithosphere under North China is

Table 2 Inferred CMB and LAB comparing with seismic Moho and LAB

Locations	Inferred CMB (km)	Inferred LAB (km)	Seismic Moho (km)	Seismic LAB (km)	Seismic data sources
West NCC	~28	>90–100	~42	90	Ma et al. (1991)
Eastern NCC	~30	~70	~30	70–80	Chen (1988)
Inland of South China	~31	>90	~31	~100	Wang et al. (1993)
Coast of South China	~31–35	~80	~28–31	75–80	Yao et al. (2006)

less well constrained, but is likely greater than that for eastern NCC (Table 2). Given the similarity of thermal gradient in western NCC and northeastern China, the lithosphere in NE China may be similar to that in Hannuoba.

There is a variation in lithospheric thickness from coastline to inland in South China. Lithosphere in Xinchang is about ~80 km thick, whereas it becomes >90 km. This spatial variation is broadly consistent with geophysical data of Ma et al. (1991), also with increasing depth of magmatic generation as suggested by Chung et al. (1994). The depth to LAB in Leizhou and Qilin is less well constrained, due to possible plume imprint in this area.

Deep Process Inferred from Variation in Thermal Gradient

Despite the difference in detail for different geologic parts, the Cenozoic lithosphere beneath eastern China is characterized by a high geothermal gradient (70–80 mW/m^2), as inferred from the geothermobarometry of garnet-bearing peridotites and pyroxenites brought by alkali basalts to the surface (Fig. 6). The high thermal gradient is in accordance with extensional tectonics in eastern China during the Cenozoic. This gradient is significantly higher than that for the lithosphere beneath North China in the Ordovician (Xu Y G, 2001). Such a contrast in thermal state for the same lithosphere at different times formed the basis of the current widely accepted concept that there was a dramatic change in lithospheric architecture during the Phanerozoic (Menzies et al., 1993; Fan and Menzies, 1992).

The surface heat flow ranging from 70–80 mW/m^2 to which the xenolith-derived Cenozoic geotherm corresponds is higher than the present-day measured values in North China (~65 mW/m^2; Wang and Wang, 1992). Such a difference may imply that the lithosphere under eastern China experienced cooling from a hotter temperature regime (Menzies and Xu, 1998), and thermal relaxation at surface is faster than in the lithospheric interior. Thermal relaxation is also recorded in basin analysis. Based on apatite fission track analyses and thermal modeling, Hu et al. (2000) showed that the heat flow in Bohai basin during the Eocene was as high as 90 mW/m^2, corresponding to the rifting stage in this region. Since the Miocene, the basin experienced a period of thermal subsidence and relaxation, resulting in the low current heat flow (64 mW/m^2).

Thermal gradient is variable in different areas in eastern China. The highest thermal gradient is observed in eastern NCC, consistent with the thinnest lithosphere in this area. A similar high geotherm can be inferred for Xinchang, along the coast of South China. Western NCC, NE China and the interior of South China are characterized by a relatively "cool" geotherm, indicative of relatively thick lithospheres under these regions. The contrast in thermal gradient and inferred lithospheric thickness in both sides of the DTGL can be attributed to the diachronous lithospheric thinning, with that in the eastern NCC significantly earlier than the Cenozoic thinning in the western NCC (Xu and Bodinier, 2004). This process eventually gave birth to the DTGL (Xu Y G, 2007).

The thermal state in South China is complex. Nevertheless, there is a decrease in thermal gradient and in lithospheric thickness from the coast to the inland. Such a variation is collaborated with westward increase in basalt's alkalinity, degree of silica undersaturation and abundance of incompatible elements and decrease in Pb isotopic ratios of Cenozoic basalt from an NE-trending extension axis in the western Taiwan Strait (Chung et al., 1994). Such a spatial chemical and isotopic variation in the basalts can be explained by different degrees of decompression melting of convecting asthenosphere under the lithosphere with different thickness (Chung et al., 1994). In this model, the spatial variation in lithosphere in South China likely resulted from lithospheric extension, probably related to the opening of the South China Sea. The greatest lithosphere thinning occurred during the Miocene beneath the axial zone at Taiwan Strait.

It appears that Cenozoic lithospheric extension only resulted in thinning of the lithosphere under the coastal regions of South China, leaving vast continental interior less affected. This is supported by restricted distribution of Cenozoic magmatism along the coastline and by thick lithosphere (>150 km) revealed by geophysical investigation. Asthenosphere-derived intraplate-type basalts were erupted during Middle Jurassic–Cretaceous in Hunan and Jiangxi

provinces and some of them carried spinel facies peridotite xenoliths (Chen et al., 2009). This indicates a relatively thin lithosphere (<80 km) in the interior of the South China continent until the Cretaceous. Therefore, there was an event leading to the thickening of the lithosphere underneath this region since the Jurassic, although the nature of this event is unclear and deserves further investigation.

CONCLUSIONS

Application of reliable thermobarometer on garnet-bearing mantle xenoliths and granulite xenoliths entrained by Cenozoic basalts in eastern China leads to the following conclusions.

(1) Two types of geotherm exist for the lithosphere beneath eastern China. The first type, as exampled by Hannuoba, Mingxi and probably NE China, is characterized by constant slope of data in the *P-T* space. The second type, as exampled by the high geotherms of Nüshan and probably Xinchang, shows variable slopes, with conductive transfer for the shallow upper mantle and advective transfer for the deep mantle.

(2) Eastern North China craton (NCC) shows a second-type geotherm, indicating a thin lithosphere (~70 km) and a thin crust (~30 km). In contrast, western NCC possesses a relatively low thermal gradient, indicative of a thick lithosphere (>90–100 km) and a thick crust-mantle transition zone. The dramatic change in crustal and mantle structure across the DTGL, also revealed by seismic studies, may have resulted from diachronous lithospheric thinning processes.

(b) There is a decrease in thermal gradient and in lithospheric thickness from the coast to the inland in South China (from ~80 km to >90 km), which is collaborated with westward variation in basalt geochemistry. This likely resulted from lithospheric extension related to the opening of the South China Sea, with the greatest lithosphere thinning during the Miocene beneath the axial zone at Taiwan Strait.

(c) The peculiar geotherm in Qilin and Leizhou peninsula is transitional between conductive and advective heat transfer. This characteristic may be related to impregnation of mantle plume on the base of the lithosphere, but further studies are needed.

ACKNOWLEDGMENTS

Thanks are due to Prof. Fuyuan Wu who encouraged us to make a synthesis on the geotherm in eastern China. This study was financially supported by the Knowledge Innovation Project of the Chinese Academy of Sciences (No. KZCX2-YW-Q08-3-6), the National Natural Science Foundation of China (Nos. 90714001, 40773015), and the CAS/SAFEA International Partnership Program for Creative Research Teams (No. KZCX2-YW-Q04-06). This is contribution No. IS-1242 from GIG-CAS.

REFERENCES CITED

Adam, J., Green, T. H., Day, R. A., 1992. An Experimental Study of Two Garnet Pyroxenite Xenoliths from the Bullenmerri and Gnotuk Maars of Western Victoria, Australia. *Contrib. Mineral. Petrol.*, 111(4): 505–514

Ai, Y., 1994. A Revision of the Garnet-Clinopyroxene Fe^{2+}-Mg Exchange Geothermometer. *Contrib. Mineral. Petrol.*, 115(4): 467–473

Akella, J., 1976. Garnet Pyroxene Equilibria in the System $CaSiO_3$-$MgSiO_3$-Al_2O_3 and in a Natural Mineral Mixture. *Am. Mineral.*, 61: 589–598

Amundsen, H. E. F., Griffin, W. L., O'Reilly, S. Y., 1987. The Lower Crust and Upper Mantle beneath Northwestern Spitsbergen: Evidence from Xenoliths and Geophysics. *Tectonophysics*, 139(3–4): 169–185

Bertrand, P., Mercier, J. C. C., 1985. The Mutual Solubility of Coexisting Ortho- and Clinopyroxene: Toward an Absolute Geothermometer for the Natural System? *Earth and Planetary Science Letters*, 77(1–2): 109–122

Brey, G. P., Köhler, T., 1990. Geothermobarometry in Four-Phase Lherzolites: II. New Thermobarometers, and Practical Assessment of Existing Thermobarometers. *Journal of Petrology*, 31(6): 1353–1378

Carswell, D. A., Gibb, F. G. F., 1987. Evaluation of Mineral Thermometers and Barometers Applicable to Garnet Lherzolite Assemblages. *Contrib. Mineral. Petrol.*, 95(4): 499–511

Chen, D. G., Li, B. X., Zhi, X. C., et al., 1994. Mineral Chemistry and REE Compositions of Peridotite Xenoliths from Liuhe, Jiangsu and Its Implications. *Acta Petrologica Sinica*, 10(1): 68–80 (in Chinese with English Abstract)

Chen, H. S., 1988. The Essentials of Geological-Geophysical Integrated Interpretation of the Line HQ-13 in the Lower Yangtze Basin on the Yangtze Metaplatform. In: Ou, Q. X.,

ed., Petroleum Exploration in Southern China. Geological Publishing House, Beijing. 239–250 (in Chinese with English Abstract)

Chen, L., Cheng, C., Wei, Z. G., 2009. Seismic Evidence for Significant Lateral Variations in Lithospheric Thickness beneath the Central and Western North China Craton. *Earth and Planetary Science Letters*, 286(1–2): 171–183

Chen, S. H., O'Reilly, S. Y., Zhou, X. H., et al., 2001. Thermal and Petrological Structure of the Lithosphere beneath Hannuoba, Sino-Korean Craton, China: Evidence from Xenoliths. *Lithos*, 56(4): 267–301

Chen, S. H., Sun, M., Zhou, X. H., et al., 1996. Pyroxenitic and Granulitic Xenoliths in Tertiary Hannuoba Basalts, Hebei Province: Petrology and *P-T* Estimation. 30th IGC (August 4–14), Beijing. 122

Chen, X. D., Lin, C. Y., Zhang, X. O., et al., 1997. Deformation Features of Mantle Xenoliths from Quaternary Basalts in Datong, Shanxi Province and Their Rheological Implications. *Seismology and Geology*, 19(4): 313–320 (in Chinese with English Abstract)

Chung, S. L., Sun, S. S., Tu, K., et al., 1994. Late Cenozoic Basaltic Volcanism around the Taiwan Strait, SE China: Product of Lithosphere-Asthenosphere Interaction during Continental Extension. *Chemical Geology*, 112(1–2): 1–20

Dawson, J. B., Smith, J. V., 1975. Occurrence of Diamond in a Mica-Garnet Lherzolite Xenolith from Kimberlite. *Nature*, 254(5501): 580–581

Ellis, D. J., Green, D. H., 1979. An Experimental Study of the Effect of Ca upon Garnet-Clinopyroxene Fe-Mg Exchange Equilibria. *Contrib. Mineral. Petrol.*, 71(1): 13–22

Fan, Q. C., Hooper, P. R., 1989. The Mineral Chemistry of Ultramafic Xenoliths of Eastern China: Implications for Upper Mantle Composition and the Paleogeotherms. *Journal of Petrology*, 30(5): 1117–1158

Fan, Q. C., Liu, R. X., Li, H. M., et al., 1998. Zircon Chronology and REE Geochemistry of Granulite Xenoliths at Hannuoba. *Chinese Sci. Bull.*, 43(2): 133–137 (in Chinese)

Fan, Q. C., Sui, J. L., Zhao, Y. W., et al., 2008. Preliminary Study on Garnet Peridotite Xenolith of Quaternary Volcanic Rocks in Middle Daxing'an Mountain Range. *Acta Petrologica Sinica*, 24(11): 2563–2568 (in Chinese with English Abstract)

Fan, W. M., Menzies, M. A., 1992. Destruction of Aged Lower Lithosphere and Asthenosphere Mantle beneath Eastern China. *Geotectonica et Metallogenia*, 16(34): 171–180

Fang, T. H., Ma, H. W., 1999. The Composition and Thermal Structure of the Upper Mantle Lithosphere beneath Kuandian Area, Liaoning Province—Implications from Mantle Xenoliths. *Geological Review*, 45(Suppl.): 450–457 (in Chinese with English Abstract)

Finnerty, A. A., Boyd, F. R., 1984. Evaluation of Thermobarometers for Garnet Peridotites. *Geochim. Cosmochim. Acta*, 48(1): 15–27

Gao, S., Rudnick, R. L., Yuan, H. L., et al., 2004. Recycling Lower Continental Crust in the North China Craton. *Nature*, 432(7019): 892–897

Green, T. H., Adam, J., 1991. Assessment of the Garnet-Clinopyroxene Fe-Mg Thermometer Using New Experimental Data. *J. Metamorph. Geol.*, 9(3): 341–347

Griffin, W. L., O'Reilly, S. Y., 1987. Is the Continental Moho the Crust-Mantle Boundary? *Geology*, 15: 241–244

Griffin, W. L., Wass, S. Y., Hollis, J. D., 1984. Ultramafic Xenoliths from Bullenmerri and Gnotuk Maars, Victoria, Australia: Petrology of a Sub-continental Crust-Mantle Transition. *Journal of Petrology*, 25(1): 53–87

Griffin, W. L., Zhang, A. D., O'Reilly, S. Y., et al., 1998. Phanerozoic Evolution of the Lithosphere beneath the Sino-Korean Craton. In: Flower, M., Chung, S. L., Lo, C. H., et al., eds., Mantle Dynamics and Plate Interactions in East Asia. Geodynamics Am. Geophys. Union, Washington D.C.. 107–126

Herzberg, C., 1978. Pyroxene Geothermometry and Geobarometry: Experimental and Thermodynamic Evaluation of Some Subsolidus Phases Relations Involving Pyroxenes in the System CaO-MgO-Al_2O_3-SiO_2. *Geochim. Cosmochim. Acta*, 42(7): 945–958

Ho, K. S., Chen, J. C., Lo, C. H., et al., 2003. ^{40}Ar-^{39}Ar Dating and Geochemical Characteristics of Late Cenozoic Basaltic Rocks from the Zhejiang-Fujian Region, SE China: Eruption Ages, Magma Evolution and Petrogenesis. *Chemical Geology*, 197(1–4): 287–318

Hu, S. B., Zhang, R. Y., Luo, Y. H., et al., 2000. Thermal History of the Bohai Basin and Its Potential for Petroleum. *China Offshore Oil and Gas* (*Geology*), 14(5): 306–314 (in Chinese with English Abstract)

Huang, X. L., Xu, Y. G., Chu, X. L., et al., 2001. Geochemical Comparative Studies of Some Granulite Terranes and Granulite Xenoliths from North China Craton. *Acta Petrologica et Mineralogica*, 20(3): 318–328 (in Chinese with English Abstract)

Huang, X. L., Xu, Y. G., Liu, D. Y., 2004. Geochronology, Petrology and Geochemistry of the Granulite Xenoliths from

Nüshan, East China: Implication for a Heterogeneous Lower Crust beneath the Sino-Korean Craton. *Geochim. Cosmochim. Acta*, 68(1): 127–149

Huang, X. L., Xu, Y. G., Lo, C. H., et al., 2007. Exsolution Lamellae in a Clinopyroxene Megacryst Aggregate from Cenozoic Basalt, Leizhou Peninsula, South China: Petrography and Chemical Evolution. *Contrib. Mineral. Petrol.*, 154(6): 691–705

Irving, A. J., 1974. Geochemical and High-Pressure Experimental Studies of Garnet Pyroxenite and Pyroxene Granulite Xenoliths from the Delegate Basaltic Pipes, Australia. *Journal of Petrology*, 15(1): 1–40

Jaques, A. L., O'Neill, H. S. C., Smith, C. B., et al., 1990. Diamondiferous Peridotite Xenoliths from the Argyle (AK1) Lamproite Pipe, Western Australia. *Contrib. Mineral. Petrol.*, 104(3): 255–276

Jin, S. Y., Pan, S. A., 1998. Mantle-Derived Xenoliths of Spinel-Garnet Lherzolite from Nüshan and Their Implications for Petrophysics. *Earth Science—Journal of China University of Geosciences*, 23(5): 475–479 (in Chinese with English Abstract)

Kennedy, C. S., Kennedy, G. C., 1976. The Equilibrium Boundary between Graphite and Diamond. *J. Geophys. Res.*, 81(14): 2467–2470

Köhler, T. P., Brey, G. P., 1990. Calcium Exchange between Olivine and Clinopyroxene Calibrated as a Geothermobarometer for Natural Peridotites from 2–60 kb with Applications. *Geochim. Cosmochim. Acta*, 54: 2375–2388

Lei, J. S., Zhao, D. P., Steinberger, B., et al., 2009. New Seismic Constraints on the Upper Mantle Structure of the Hainan Plume. *Physics of the Earth and Planetary Interiors*, 173(1–2): 33–50

Lin, C. Y., Huang, X. L., Xu, Y. G., et al., 2003. Thermal Structure and Rheology of Upper Mantle beneath Leizhou Peninsula, Guangdong Province. *China Journal of Tropical Oceanography*, 22(2): 49–62 (in Chinese with English Abstract)

Lin, C. Y., Shi, L. B., Chen, X. D., et al., 1995. Rheological Features of Garnet Lherzolite Xenoliths from Xinchang, Zhejiang Province, China and Their Geological Implications. *Acta Petrologica Sinica*, 11(1): 55–64 (in Chinese with English Abstract)

Lin, C. Y., Shi, L. B., Chen, X. D., et al., 1999. Thermal Structure and Rheology of the Upper Mantle beneath Mingxi, Fujian Province. *Geological Review*, 45(4): 352–360 (in Chinese with English Abstract)

Lin, C. Y., Shi, L. B., Han, X. L., et al., 1998. Thermal Structure and Rheology of the Upper Mantle beneath Zhejiang Province. *Science in China* (*Series D*), 28(2): 97–104

Liu, J. H., Yan, J., 2007. Peridotitic Xenoliths in the Cenozoic Basalts from the Subei Basin. *J. Mineral. Petrol.*, 27(2): 39–46 (in Chinese with English Abstract)

Liu, R. X., Chen, W. J., Sun, J. Z., et al., 1992. The K-Ar Age and Tectonic Environment of Cenozoic Volcanic Rock in China. In: Liu, R. X., ed., The Age and Geochemistry of Cenozoic Volcanic Rock in China. Seismological Press, Beijing. 1–43 (in Chinese)

Ma, L. F., Qiao, X. F., Min, L. R., et al., 2002. Geological Atlas of China. Geological Publishing House, Beijing (in Chinese)

Ma, X. Y., Liu, C. Q., Liu, G. D., 1991. Xiangshui (Jiangsu Province) to Mandal (Inner Mongolian) Geoscience Transect. *Acta Geologica Sinica*, 65(3): 199–215 (in Chinese with English Abstract)

McCarthy, T. C., Patiño-Douce, A. E., 1998. Empirical Calibration of the Silica-Ca-Tschermak's-Anorthite (SCAn) Geobarometer. *J. Metamorph. Geol.*, 16(5): 675–686

McKenzie, D., Bickle, M. J., 1988. The Volume and Composition of Melt Generated by Extension of the Lithosphere. *Journal of Petrology*, 29(3): 625–679

Menzies, M. A., Fan, W. M., Zhang, M., 1993. Palaeozoic and Cenozoic Lithoprobes and the Loss of >120 km of Archean Lithosphere, Sino-Korean Craton, China. In: Prichard, H. M., Alabaster, T., Harris, N. B. W., et al., eds., Magmatic Processes and Plate Tectonics. *Geological Society of London Special Publication*, 76: 71–81

Menzies, M. A., Xu, Y. G., 1998. Geodynamics of the North China Craton. In: Flower, M. F. J., Chung, S. L., Lo, C. H., et al., eds., Mantle Dynamics and Plate Interactions in East Asia. *Geodynamics Am. Geophys. Union, Washington, DC*, 27: 155–164

Mori, T., Green, D. H., 1978. Laboratory Duplication of Phase Equilibria Observed in Natural Garnet Lherzolites. *J. Geol.*, 86(1): 83–97

Nickel, H. G., Green, D. H., 1985. Empirical Geothermobarometry for Garnet Peridotites and Implications for the Nature of the Lithosphere, Kimberlites and Diamonds. *Earth Planet. Sci. Lett.*, 73(1): 158–170

Nixon, P. H., Boyd, F. R., 1973. Petrogenesis of the Granular and Sheared Ultrabasic Nodule Suite in Kimberlites. In: Nixon, P. H., ed., Lesotho Kimberlites. Lesotho National Development Corporation, Lesotho. 48–56

O'Neill, H. S. C., 1981. The Transition between Spinel Lherzolite and Garnet Lherzolite, and Its Use as a Geobarometer. *Contrib. Mineral. Petrol.*, 77(2): 185–194

O'Reilly, S. Y., Griffin, W. L., 1985. A Xenolith Derived Geotherm for Southeastern Australia and Its Geophysical Implications. *Tectonophysics*, 111(1–2): 41–63

O'Reilly, S. Y., Griffin, W. L., 1996. 4-D Lithosphere Mapping: Methodology and Examples. *Tectonophysics*, 262(1–4): 3–18

Pearson, D. G., Boyd, F. R., Haggerty, S. E., et al., 1994. The Characterisation and Origin of Graphite in Cratonic Lithospheric Mantle: A Petrological Carbon Isotope and Raman Spectroscopic Study. *Contrib. Mineral. Petrol.*, 115(4): 449–466

Pokhilenko, N. P., Sobolev, N. V., Lavrent'ev, Y. G., 1977. Xenoliths of Diamondiferous Ultramafic Rocks from Yakutian Kimberlites. 2nd Int. Kimberlite Conf., Am. Geophys. Union, Washington D.C.

Qi, Q., Taylor, L., Zhou, X., 1995. Petrology and Geochemistry of Mantle Peridotite Xenoliths from SE China. *Journal of Petrology*, 36(1): 55–79

Robinson, J. A. C., Wood, B. J., 1998. The Depth of the Spinel to Garnet Transition at the Peridotite Solidus. *Earth and Planetary Science Letters*, 164(1–2): 277–284

Sachtleben, T., Seck, H. A., 1981. Chemical Control of Al-Solubility in Orthopyroxene and Its Implications on Pyroxene Geothermometry. *Contrib. Mineral. Petrol.*, 78(2): 157–165

Shee, S. R., Gurney, J. J., Robinson, D. N., 1982. Two Diamond-Bearing Peridotite Xenoliths from the Finsch Kimberlite, South Africa. *Contrib. Mineral. Petrol.*, 81(2): 79–87

Shi, L. B., Lin, C. Y., Chen, X. D., et a1., 2000. A Xenolith-Derived Geotherm for the Lower Crust and Upper Mantle beneath Hanuoba Area, Hebei Province, China and Its Geological Implications. *Seismology and Geology*, 22(1): 37–46 (in Chinese with English Abstract)

Su, B. X., Zhang, H. F., Wang, Q. Y., et al., 2007. Spinel-Garnet Phase Transition Zone of Cenozoic Lithospheric Mantle beneath the Eastern China and Western Qinling and Its *T-P* Condition. *Acta Petrologica Sinica*, 23(6): 1313–1320 (in Chinese with English Abstract)

Tsai, H. M., Meyer, H. O. A., Moreau, J., et al., 1979. Mineral Inclusions in Diamond: Premier, Jagersfontein and Finsch Kimberlites, South Africa and Williamson Mine, Tanzania. In: Boyd, F. R., Meyer, H. O. A., eds., Kimberlites, Diatremes and Diamonds: Their Geology, Petrology and Geochemistry. *Proceedings of the International Kimberlite Conference*, 16–26

Wang, J. A., Wang, J. Y., 1992. The Thermal Evolution and Thermal Structure of Lithosphere in Coastal Region, Southeast China. In: Li, J. L., ed., The Study on Evolution and Structure of the Ocean-Continental Lithosphere, Southeast China. China Sci. Techni. Publ. House, Beijing. 302–315 (in Chinese)

Wang, L. C., 1996. Occurrence of the Dashihe Olivine Deposit in Jilin Province, China. *Journal of Changchun University of Geology*, 26(1): 43–46 (in Chinese with English Abstract)

Wang, P. Z., Chen, Y. A., Cao, B. T., et al., 1993. Crust-Upper Mantle Structure and Deep Structural Setting of Fujian Province. *Geology of Fujian*, 12(2): 79–158 (in Chinese)

Werling, F., Altherr, R., 1997. Thermal Evolution of the Lithosphere beneath the French Massif Central as Deduced from Geothermobarometry on Mantle Xenoliths. *Tectonophysics*, 275(1–3): 119–141

Wilde, S., Zhou, X. H., Nemchin, A. A., et al., 2003. Mesozoic Crust-Mantle Interaction beneath the North China Craton: A Consequence of the Dispersal of Gondwanaland and Accretion of Asia. *Geology*, 31: 817–820

Witt-Eickschen, G., Seck, H. A., 1991. Solubility of Ca and Al in Orthopyroxene from Spinel Peridotite: An Improved Version of an Empirical Geothermometer. *Contrib. Mineral. Petrol.*, 106(4): 431–439

Wood, B. J., 1974. The Solubility of Alumina in Orthopyroxene Coexisting with Garnet. *Contrib. Mineral. Petrol.*, 46(1): 1–15

Xu, X. S., O'Reilly, S. Y., Griffin. W. L., 1999. The Geotherm of the Lithosphere beneath Qilin, SE China: A Reappraisal and Implications for *P-T* Estimation of Fe-Rich Pyroxenites: Reply. *Lithos*, 47(3–4): 195–199

Xu, X. S., O'Reilly, S. Y., Griffin, W. L., et al., 1998. The Nature of the Cenozoic Lithosphere at Nüshan, Eastern China. In: Flower, M., Chung, S. L., Lo, C. H., et al., eds., Mantle Dynamics and Plate Interactions in East Asia. *Geodynamics Series*, 27: 167–195

Xu, X. S., O'Reilly, S. Y., Zhou, X. M., et al., 1996. A Xenolith-Derived Geotherm and the Crust-Mantle Boundary at Qilin, Southeastern China. *Lithos*, 38(1–2): 41–62

Xu, Y. G., 1993. Geothermometers Applicable to the Mantle Xenoliths. *Acta Petrologica Sinica*, 9(2): 167–180 (in Chinese with English Abstract)

Xu, Y. G., Menzies, M. A., Thirlwall, M. F., et al., 2003. "Reactive" Harzburgites from Huinan, NE China: Products of Lithosphere-Asthenosphere Interaction during Lithospheric Thinning? *Geochimica et Cosmochimca Acta*, 67(3): 487–505

Xu, Y. G., 2001. Evidence for Crustal Components in Mantle Source and Constraints on Recycling Mechanism: Pyroxenite Xenoliths from Hannuoba, North China. *Physics and Chemistry of the Earth*, 26: 747–757

Xu, Y. G., 2002. Evidence for Crustal Components in the Mantle Source and Constraints on Recycling Mechanisms: Pyroxenite Xenoliths from Hannuoba, North China. *Chemical Geology*, 182(2–4): 301–322

Xu, Y. G., 2007. Diachronous Lithospheric Thinning of the North China Craton and Formation of the Daxing'anling-Taihangshan Gravity Lineament. *Lithos*, 96(1–2): 281–298

Xu, Y. G., Bodinier, J. L., 2004. Contrasting Enrichment in High- and Low-Temperature Mantle Xenoliths from Nüshan, Eastern China: Results of a Single Metasomatic Event during Lithospheric Accretion? *J. Petrol.*, 45(2): 321–341

Xu, Y. G., Lin, C. Y., Shi, L. B., 1999. The Geotherm of the Lithosphere beneath Qilin, SE China: A Re-appraisal and Implications for *P-T* Estimation of Fe-Rich Pyroxenites. *Lithos*, 47(3–4): 181–193

Xu, Y. G., Lin, C. Y., Shi, L. B., et al., 1995. A Petrological Paleogeotherm of the Upper Mantle of Eastern China and Its Geological Implications. *Science in China* (*Series B*), 25(8): 874–881 (in Chinese)

Xu, Y. G., Mentzies, M. A., Vroon, P., et al., 1998. Texture-Temperature-Geochemistry Relationship in the Upper Mantle as Revealed from Spinel Peridotite Xenoliths from Wangqing, NE China. *Journal of Petrology*, 39(3): 469–493

Xu, Y. G., Ross, J. V., Mercier, J. C. C., 1993. The Upper Mantle beneath the Continental Rift of Tanlu, Eastern China: Evidence for the Intra-lithospheric Shear Zones. *Tectonophysics*, 225(4): 337–360

Yao, B. C., Wan, L., Zeng, W. J., et al., 2006. The Three-Dimensional Structure of Lithosphere and Its Evolution in the South China Sea. Geological Publishing House, Beijing. 1–233 (in Chinese)

Ye, S., Yang, M., Ye, D. L., et al., 2001. Rb-Sr Isotopic Dating and Significance of a Kimberlitic Lamprophyre Pipe in Lujing, Anyuan, Jiangxi Province. *Geological Science and Technology Information*, 20(2): 27–29 (in Chinese with English Abstract)

Yu, J. H., O'Reilly, S. Y., Griffin, W. L., et al., 2003. The Thermal State and Composition of the Lithospheric Mantle beneath the Leizhou Peninsula South China. *J. Volcanol. Geotherm. Res.*, 122(3–4): 165–189

Yu, S. Y., 2008. Petrology and Geochemistry of Mantle-Derived Xenoliths in Cenozoic Basalts from Shuangliao and Jiaohe: Constraints on the Nature and Evolution of the Lithospheric Mantle beneath Northeastern China: [Dissertation]. Graduate University of Chinese Academy of Sciences, Beijing. 1–138 (in Chinese with English Abstract)

Yu, X. H., Mo, X. X., Liao, Z. L., et al., 2001. Temperature-Pressures of the Garnet-Bearing Lherzolite and Pyroxenite Xenoliths from Western Qinling, China. *Science in China* (*Series D*), 31(Suppl.): 128–133 (in Chinese)

Yu, X. H., Zhao, Z. D., Mo, X. X., et al., 2005. $^{40}Ar/^{39}Ar$ Dating for Cenozoic Kamafugites from Western Qinling in Gansu Province. *Chinese Science Bulletin*, 50(23): 2638–2643 (in Chinese)

Zheng, J. P., O'Reilly, S. Y., Griffin, W. L., et al., 2004. Nature and Evolution of Mesozoic–Cenozoic Lithospheric Mantle beneath the Cathaysia Block, SE China. *Lithos*, 74(1–2): 41–65

Zheng, J. P., O'Reilly, S. Y., Griffin, W. L., et al., 2001. Relict Refractory Mantle beneath the Eastern North China Block: Significance for Lithosphere Evolution. *Lithos*, 57(1): 43–66

Zheng, J. P., O'Reilly, S. Y., Griffin, W. L., et al., 1998. Nature and Evolution of Cenozoic Lithospheric Mantle beneath Shandong Peninsula, Sino-Korean Craton. *Int. Geol. Rev.*, 40(6): 471–499

Zheng, J. P., Griffin, W. L., O'Reilly, S. Y., et al., 2006. Mineral Chemistry of Peridotites from Paleozoic, Mesozoic and Cenozoic Lithosphere: Constraints on Mantle Evolution beneath Eastern China. *Journal of Petrology*, 47(11): 2233–2256